Acta Cryst. (1977). A**33**, 593–601

X-ray Measurement of the Root-Mean-Square Displacement of Atoms in Zinc Single Crystals. A Case of High Anisotropic Extinction

BY ELISABETH ROSSMANITH

Mineralogisch-Petrographisches Institut, Universität Hamburg, Grindelallee 48, 2000 *Hamburg* 13, *Federal Republic of Germany*

(*Received* 13 *October* 1976; *accepted* 15 *February* 1977)

The thermal parameters of Zn have been refined by the use of Bragg reflexions measured with Mo $K\alpha$ and Cu $K\alpha$ radiation for one temperature only. Several models of the anisotropic extinction correction have been examined. It is shown that the use of the extinction correction strongly influences the values of the thermal parameters. These parameters are however only slightly affected by the choice of extinction correction model. The programs *LINEX* 74 and *ORXFLS* 3 were used for refinement, the latter in a version modified by the author. The best fit was obtained by using the *LINEX* 74 type I model with a Lorentzian distribution of the mosaic spread and the Thornley–Nelmes model for the ellipsoid of the anisotropic mosaic spread. The result for the root-mean-square displacement was $u_a = 0{\cdot}098 \pm 0{\cdot}001$ Å (Mo $K\alpha$ radiation), $u_a = 0{\cdot}102 \pm 0{\cdot}006$ Å (Cu $K\alpha$ radiation) in the a direction of the lattice and $u_c = 0{\cdot}161 \pm 0{\cdot}004$ Å (for both radiations) in the c direction. These results are in good agreement with those of Skelton & Katz [*Phys. Rev.* (1968), **171**, 801–808], measured in a temperature range from 4·85 to 600 K.

Introduction

During the last decade the validity of the temperature factors β_{ij} calculated from X-ray Bragg intensity measurements on single crystals with least-squares routines has been questioned. To obtain an answer about the quality of these temperature factors two projects were started: (*a*) The American Crystallographic Association asked seven institutes to measure the highly symmetric CaF_2 single crystal. Each institute in turn received the same CaF_2 crystal for measurement (Abrahams *et al.*, 1967). (*b*) The International Union of Crystallography asked 16 different institutes to measure one of 16 different D-(+)-tartaric acid single crystals (Abrahams, Hamilton & Mathieson, 1970; Hamilton & Abrahams, 1970). These two projects and the results of comparing measured and calculated temperature factors of Ni ($B_{\text{X-ray}} = 0{\cdot}37$ Å^2, $B_{\text{neutron}} = 0{\cdot}43$ Å^2, $B_{\text{theor.}} = 0{\cdot}38$ Å^2) and Al ($B_{\text{X-ray}} = 0{\cdot}85$ Å^2, $B_{\text{neutron}} = 0{\cdot}89$ Å^2, $B_{\text{theor.}} = 0{\cdot}87$ Å^2) (Willis & Pryor, 1975, and references cited therein) leads to the following conclusion: In the case of low symmetrical single crystals built up of light atoms [project (*b*)], there is striking disagreement for the β_{ij} between the results given by different authors. In the worst case in project (*b*) the temperature factors disagree by a factor of 10. In the case of highly symmetrical substances [project (*a*) and values for Ni and Al], built up of heavy atoms in special positions, for which the six temperature factors reduce to one or two independent parameters, there is satisfactory agreement between different measurements and between measured and calculated temperature factors. These results encouraged the author to estimate the temperature factors of Zn using the intensities measured in Bragg positions of a Zn single crystal for one temperature only.

Temperature factors calculated by least-squares analysis are strongly dependent on whether the absorption correction, the extinction correction and the correction for TDS are properly applied. Ignoring one, two or all of these corrections leads to an underestimate of temperature factors. In this investigation absorption correction was used and the extinction was studied extensively; the TDS correction was, however, not made.

Previous work on Zn root-mean-square displacement

Previous work is collated in Table 1. With the help of calculated values for u_a and u_c Brindley (1936) corrected the measured form factor of the Zn atom and compared the result with calculated form-factor values. The comparison led him to the conclusion that his calculated values for u_a and u_c must be too small. In subsequent papers, by Jauncey & Bruce (1936) and Wollan & Harvey (1937), larger values for u_a and u_c were estimated (Table 1). The relatively small values found by Ryba (1960) may be because he used a large single crystal ($10 \times 25 \times 1{\cdot}5$ mm) and did not correct his intensities for extinction, particularly as the mosaic structure (which is irreversibly temperature dependent) governs the extinction correction.

Experimental

A sphere of Zn single crystal (99·9999% Zn), obtained by the extrusion of molten zinc through a narrow oil-

Table 1. *Previous work on the root-mean-square displacement of* Zn

u_a and u_c are the mean atomic displacements in directions **a** and **c** of the crystal lattice.

Author	Method to estimate u_a and u_c	u_a (Å) $T=293$ °K	u_c (Å)
Zener (1936)	Calculated	0·0636	0·0853
Brindley (1936)	Calculated	0·0791	0·1265
Jauncey & Bruce (1936)	From measurements of diffuse scattering on Zn single crystals	0·093	0·172
Wollan & Harvey (1937)	From measurements of Bragg intensities on Zn powder sample for two temperatures	0·0913	0·153
Ryba (1960)	From measurements of 400 and 006 reflexions on Zn single crystal in the temperature range 13°–400 °C	0·077	0·128
Skelton & Katz (1968)	From measurements of 004, 006, 008, 300, 400, 600 and 210 reflexions on Zn single crystals in the temperature range 4·85°–600 °K	0·106	0·161

encased tube was supplied by Guse (1971). Oil and molten zinc are contained within a large glass column which has a temperature gradient from the top to the bottom. The extruded zinc solidifies into spherical droplets as they fall through the oil. Most of the spheres are single crystals, although under some conditions polycrystalline phases also develop. The mean radius $R_s=0{\cdot}00680\pm0{\cdot}00018$ cm of the Zn sample was obtained by measuring it ten times in various orientations. The values of $\mu_0 R_s$ obtained for Mo $K\alpha$ and Cu $K\alpha$ for this sphere are therefore 2·69 and 2·92 respectively.

Zinc crystallizes in the well known h.c. packing, space group $P6_3/mmc$ (No. 194) with two atoms per unit cell in the special positions 0,0,0 and $\frac{2}{3},\frac{1}{3},\frac{1}{2}$.

The intensities of all reflexions in one hemisphere with $\sin\theta/\lambda<0{\cdot}617$ Å^{-1} were measured with Cu $K\alpha$ radiation on a Siemens AED four-circle diffractometer with graphite monochromator. The reflexions were measured by the five-point method, where the integrated intensity I_m is given by

$$I_m=(I_1+I_3+I_5)/2-(I_2+I_4)\,,$$

where I_1 is the scan from peak maximum to the left end of the scan range, I_3 is the scan from the left end to the right end of the scan range, I_5 is the scan from the right end of the scan range to peak maximum and I_2 and I_4 are stationary registrations of background. Each reflexion was measured five times; the mean value of these five measurements was used in further calculations. Twenty of the 99 reflexions are symmetrically independent.

The unit-cell dimensions were estimated by least-squares analysis using the reflexion positions for both Cu $K\alpha_1$ ($\lambda=1{\cdot}54433$ Å) and Cu $K\alpha_2$ ($\lambda=1{\cdot}54051$ Å) radiation: $a=b=2{\cdot}6659\pm0{\cdot}0001$, $c=4{\cdot}9403\pm0{\cdot}0002$ Å, compared with values obtained by Lynch & Drickamer (1965): $a=b=2{\cdot}665$, $c=4{\cdot}947$ Å.

The sample was measured once more with a Hilger and Watts diffractometer with graphite monochromator. Mo $K\alpha$ was used to measure all reflexions in one sixth of the hemisphere with $\sin\theta/\lambda<0{\cdot}809$ Å^{-1} in $\theta/2\theta$ scan. The Friedel pairs were also measured. The mean of the intensities of hkl and $\bar{h}\bar{k}\bar{l}$ was used in later calculations. Of the 63 reflexions 36 are symmetrically independent. All intensities were corrected for absorption with the absorption factor A^* for spheres of Weber (1969). The Lp correction was applied with the formula given by Azaroff (1955) in the case where the scattering planes of the monochromator and the sample are mutually perpendicular.

Extinction correction: theoretical work

With the two least-squares programs *ORXFLS*3 and *LINEX* 74 [both are modified versions of *ORFLS* by Busing, Martin & Levy (1962)] it is possible to correct the intensity data for anisotropic secondary extinction. The program *ORXFLS*3 uses the extinction formula given by Zachariasen (1967) and modified by Coppens & Hamilton (1970). *LINEX* 74 incorporates the extinction treatment of Becker & Coppens (1974, 1975). The extinction correction y is defined by

$$I/y=I_k$$

where I is the measured integrated intensity, corrected for absorption and Lp and I_k is the intensity in the kinematical approximation. The results for y for a mosaic crystal containing spherical domains of radius r with a Gaussian distribution for both the mosaic spread and the mean diffracting unit cross section inside the mosaic crystal (Zachariasen, 1967) are shown in Table 2 together with the results of Becker & Coppens (1974). Various authors had pointed out shortcomings of Zachariasen's extinction correction and Becker & Coppens therefore carefully reconsidered his calculations with both Gaussian and Lorentzian distributions for the mosaic spread and the mean diffracting unit cross section.

For unpolarized X-ray beams

$$y=\frac{y_\perp+y_\parallel\cos^2 2\theta}{1+\cos^2 2\theta} \tag{1}$$

has to be used, where $y_\perp=y(P=1)$ and $y_\parallel=y(P=\cos^2 2\theta)$. If the value of $Q_0\,\overline{T}_\mu g^*$ is smaller than 5, the approximation

$$y=\frac{1}{\left[1+2Q_0\,\overline{T}_\mu g^*\,\dfrac{1+\cos^4 2\theta}{1+\cos^2 2\theta}\right]^{1/2}} \tag{2}$$

can be used for an unpolarized X-ray beam.

If the diffractometer is used with a monochromator, then y is given by

$$y=\frac{y_{\perp}\cos^2 2\theta_M+y_{\parallel}\cos^2 2\theta}{\cos^2 2\theta_M+\cos^2 2\theta}. \qquad (3)$$

The parameters r and g in Table 2 are isotropic. Several models have been developed for r and g anisotropic. In type I crystals the mosaic spread is dependent on the direction in the crystal. Therefore Coppens & Hamilton (1970) replaced g by $g(\mathbf{D})$, where $\mathbf{D}$ is the unit vector normal to the diffraction plane. For type II crystals the mosaic blocks are no longer spheres but ellipsoids. Coppens & Hamilton (1970) then replaced r by $r(\mathbf{N})$, where $\mathbf{N}$ is the unit vector which lies in the diffraction plane and is perpendicular to the incident beam. Becker & Coppens (1975) replaced r by $r(\mathbf{u})$, where $\mathbf{u}$ is the unit vector along the incident beam. The models of anisotropy are collated in Table 3. In deriving y as defined in Table 2, it was assumed that absorption of X-rays in the crystal is small ($\mu\bar{T}<1$). Following Zachariasen (1968*b*), it is necessary to allow for the Borrmann effect when extinction is high and $\mu\bar{T}>1$. The Borrmann effect describes the fact that, if the Laue–Bragg equation is exactly or nearly satisfied, μ is no longer the linear absorption coefficient μ_0 in the direction of Bragg reflexion, but

$$\mu=\mu_0\pm K\mu_H\kappa_K$$

with

$$\mu_H=[(\sum_j \mu_{aj})/V]\exp[2\pi i(hx_j+ky_j+lz_j)]\exp(-M);$$

for $z<1$:

$$\kappa_K=z/[\pi(1-z^2)^{-1/2}]\times\ln[(1+(1-z^2)^{1/2}]/[1-(1-z^2)^{1/2}],$$

for $z\geq 1$:

$$\kappa_K=2/\pi,$$

$$z=[2r^*K|F|(e^2/mc^2)\lambda]/(V\sin 2\theta). \qquad (4)$$

$K=1$ for the normal and $K=|\cos 2\theta|$ for the parallel component of polarization.

Using this μ in deriving the extinction correction, we get a weighted y:

$$y=\frac{A_{+1}y_{+1}+A_{-1}y_{-1}+K^2(A_{+K}y_{+K}+A_{-K}y_{-K})}{2A_0(1+K^2)} \qquad (5)$$

where A is the transmission factor ($A=1/A^*$) and the indices have the meaning: $0\ldots\mu_0$; $\pm 1\ldots\mu_0\pm u_H\kappa_1$; $\pm K\ldots\mu_0\pm K\mu_H\kappa_K$.

Table 2. *Extinction correction for X-rays polarized perpendicular* ($P=1$) *and parallel* ($P=\cos^2 2\theta$) *to the scattering plane*

The symbols used are defined in the Appendix.

Zachariasen (1967) Gaussian distribution	Becker & Coppens (1974) Gaussian distribution	Lorentzian distribution
	$W_G(\Delta)=(2g)^{1/2}\exp(-2\pi g^2\Delta^2)$	$W_L(\Delta)=2g/(1+4\pi^2\Delta^2g^2)$
$y=(1+2x)^{-1/2}$	$y=\left[1+2{\cdot}12x+\frac{A(\theta)x^2}{1+B(\theta)x}\right]^{-1/2}$	$y=\left[1+2x+\frac{A(\theta)x^2}{1+B(\theta)x}\right]^{-1/2}$
	$x=Q_0P\,\bar{T}_\mu g^*;\ \bar{T}_\mu=(1/A^*)\,(\mathrm{d}A^*/\mathrm{d}\mu)$	
$g^*=(r/\lambda)\,[1+(r/\lambda g)^2]^{-1/2}$	$g^*=\frac{r\sin 2\theta}{\lambda}\left[1+\frac{9}{8}\left(\frac{r\sin 2\theta}{\lambda g}\right)^2\right]^{-1/2}$	$g^*=\frac{r\sin 2\theta}{\lambda}\left(1+\frac{r\sin 2\theta}{\lambda g}\right)^{-1}$
Type I: g small: Extinction depends on the mosaic spread parameter η only.		
$g^*=g$	$g^*\simeq g$	$g^*=g$
Type II: g large: Extinction depends on mosaic block size only.		
$g^*=r/\lambda$	$g^*=r\sin 2\theta/\lambda$	$g^*=r\sin 2\theta/\lambda$

Table 3. *The models of anisotropy of* η *and* r

$\mathbf{Z}$, $\mathbf{Y}$, $\mathbf{W}$ and $\mathbf{E}$ are second-order tensors. r and λ in Å, η in seconds.

Type I	Coppens & Hamilton (1970)	Thornley & Nelmes (1974)
Gaussian	$\eta(\mathbf{D})=\frac{1}{2\pi^{1/2}g(\mathbf{D})}=\frac{58186}{(\mathbf{D}'\mathbf{Z}\mathbf{D})^{1/2}}$	$\eta(\mathbf{D})=\frac{(\mathbf{D}'\mathbf{Z}\mathbf{D})^{1/2}}{2\pi^{1/2}}=58186(\mathbf{D}'\mathbf{Y}\mathbf{D})^{1/2}$
Lorentzian	$\eta(\mathbf{D})=\frac{1}{2\pi g(\mathbf{D})}=\frac{32830}{(\mathbf{D}'\mathbf{Z}\mathbf{D})^{1/2}}$	$\eta(\mathbf{D})=\frac{(\mathbf{D}'\mathbf{Y}\mathbf{D})^{1/2}}{2\pi}=32830\,(\mathbf{D}'\mathbf{Y}\mathbf{D})^{1/2}$
Type II	Coppens & Hamilton (1970)	Becker & Coppens (1975)
	$r(\mathbf{N})=10^4\lambda/(\mathbf{N}'\mathbf{W}\mathbf{N})^{1/2}$	$r(\mathbf{u})=10^4\lambda/(\mathbf{u}'\mathbf{E}\mathbf{u})^{1/2}$

Extinction correction: calculation and results of this work

As input data for *ORXFLS*3 and *LINEX* 74 we used the atom form factors for Zn^{2+} of Cromer & Mann (1968) and the values for anomalous dispersion for Zn of Cromer & Libermann (1970). Because of the high symmetry of h.c.p. Zn the six temperature factors β_{ij} are constrained (Peterse & Palm, 1966):

$$\beta_{11}=\beta_{22},\ \beta_{12}=\beta_{11}/2,\ \beta_{23}=\beta_{13}=0\,.$$

The refinement was first carried out with the scale factor K_1 and the two independent temperature factors β_{11} and β_{33} varying. Then the isotropic extinction parameter was varied together with the scale factor and the temperature factors. At the end of the refinement by least-squares analysis the scale factor, the two temperature factors and the six extinction parameters for anisotropic extinction were refined simultaneously. The results for *wR* for these three steps of refinement using *ORXFLS*3 are 0·10, 0·057 and 0·030 respectively. Using the significance test of Hamilton (1965), we can therefore reject the hypothesis that extinction correction is isotropic on a significance level of $\alpha=$ 0·005.

(*a*) *The results of refinement with ORXFLS*3

In *ORXFLS*3 the formulae for y of Zachariasen (1967) (Table 2) together with formula (2) are used. Anisotropic extinction parameters can be refined on the basis of the models of anisotropy for type I (Gaussian only) and type II crystals of Coppens & Hamilton (1970) (Table 3).*

Two modifications were made in *ORXFLS*3: Firstly we can either use the original *ORXFLS*3 formula for y for an unpolarized incident beam, or take into account the influence of the monochromator (equation 3). Secondly we can calculate y with or without considering the Borrmann effect. To calculate y including the Borrmann effect defined in (5), it is necessary to calculate for each *hkl* the transmission factor A and the absorption-weighted mean path length $\overline{T}_\mu$ for each of the five different μ defined in (4). This is done with the help of two additional subroutines in *ORXFLS*3. In the first subroutine the five different μ values are calculated for each *hkl* with formula (4). With the second subroutine, in which the absorption factor table of Weber (1969) is incorporated, it is possible to calculate the five different values for A and A^* ($A=1/A^*$) and the five different $\overline{T}_\mu$ values with $\overline{T}_\mu=(1/A^*)(\mathrm{d}A^*/\mathrm{d}\mu)$. y and the derivatives of the structure factor with respect to the extinction parameters were modified in *ORXFLS*3

The results of refinement with *ORXFLS*3 are shown in the upper part of Table 4 for the Cu $K\alpha$ measurement and in the upper part of Table 5 for the Mo $K\alpha$ measurement. In the second column the number of the calculation is given. The third column in both tables indicates the type of extinction correction applied, type I or type II as defined by Zachariasen. The values for the refined tensor components Z_{ij}, Y_{ij} for type I and W_{ij}, E_{ij} for type II are tabulated in the fifth column. In the last two columns information is given as to whether the calculations were made including the Borrmann effect or not, and whether (2) or (3) was used to calculate y.

Effect of including the Borrmann effect

The Borrmann effect is important for perfectly grown single crystals with high absorption. It is generally considered that metals do not form perfectly grown single crystals. But for a thick Zn single crystal Merlini & Pace (1965) measured the Borrmann effect for the 002 reflexion. This result and the fact that $\mu R_s>1$ for our Zn sample encouraged the author to include the Borrmann effect in extinction correction for the Zn sphere. Results of calculations which include the Borrmann effect are seen in Tables 4 and 5 in the third and fourth rows. The R values for least-squares analysis including the Borrmann effect are much higher than without the Borrmann effect for both Cu and Mo. It is therefore concluded that formula (5) does not adequately describe the extinction in the Zn sample.

Effect of polarization

The effect of using the extinction correction with the polarization of the X-ray beam taken into account is more pronounced for Cu $K\alpha$ measurements than for Mo $K\alpha$ measurements. This is not surprising, because $\cos 2\theta_M=0{\cdot}89$ for Cu radiation for the Siemens AED and $\cos 2\theta_M=0{\cdot}98$ for Mo radiation for the Hilger and Watts diffractometer [for $\cos 2\theta_M=1$ (3) is identical with (1) for an unpolarized incident beam]. In what follows calculations not including the Borrmann effect in Tables 4 and 5 are considered. It can be seen that neglect of polarization has small influence on the R value and on the thermal vibration amplitudes u_a and u_c (listed in the fourth column of the Tables 4 and 5), but is important for the results on the mosaic block size r_{ii}. [These principal axes r_{ii} and the direction cosines with respect to the orthogonal system with axes parallel to **a**, **a** × **c** and **c** are given in the fifth column of Tables 4 and 5 together with the tensor components for calculations (5), (6), (16) and (17).] This implies that the use of the unmodified *ORXFLS*3 version to correct intensity data measured with a diffractometer with monochromator will give erroneous extinction parameters.

Type I *or type* II *– comparison of* Mo *and* Cu *data*

In using the type I model in *ORXFLS*3 non-positive-definite values for the extinction parameters are obtained for both Cu and Mo.

For the type II model of anisotropy the results

* The tensor components are given in the orthogonal system with axes parallel to **a**, **a** × **c** and **c**.

Table 4. Cu *data*: *results of refinement for different anisotropic extinction correction models*

T_{ij}: tensor components Z_{ij}, W_{ij}, Y_{ij} and E_{ij} respectively.

Program used	No.	Type	u_a ($\times 10^3$) u_c ($\times 10^3$)	T_{11}	T_{22}	T_{33}	T_{12}	T_{13}	T_{23}	R ($\times 10^3$) wR ($\times 10^3$)	K_1	σ	B.E.*	Using (2) or (3)
*ORXFLS*3	1	I	103 (8) 159 (6)	not positive-definite						57 57	157·5 ±11·3	3·12	yes	(2)
	2	I	102 (8) 156 (6)	not positive-definite						36 44	148·0 ±6·4	2·38	no	(2)
	3	II	090 (7) 155 (6)	2·57 ±1·07	2·48 ±1·00	50·5 ±21·8	0·20 ±0·36	0·65 ±1·5	0·53 ±1·4	43 46	151·8 ±7·2	2·50	yes	(2)
	4	II	091 (12) 154 (9)	1·12 ±0·69	1·04 ±0·63	14·1 ±9·2	0·05 ±0·17	0·24 ±0·58	0·16 ±0·53	56 59	159·2 ±12·2	3·19	yes	(3)
	5	II	093 (5) 153 (4)	9·35 ±2·4	9·80 ±2·4	167·3 ±44·5	0·38 ±0·98	2·19 ±4·11	1·53 ±3·96	26 30	144·2 ±3·8	1·64	no	(2)
				5·1 (7) 4·9 (7) 1·2 (2)	0·88 0·47 −0·01	0·47 −0·88 0·01	0·00† 0·01 1·00							
	6	II	101 (4) 161 (3)	4·25 ±0·86	4·33 ±0·80	74·9 ±15·5	0·18 ±0·35	0·89 ±1·5	0·61 ±1·5	27 32	154·6 ±4·0	1·76	no	(3)
				7·6 (8) 7·3 (7) 1·8 (2)	0·79 0·62 −0·01	0·62 −0·79 0·01	0·00† 0·01 1·00							

Program used	No.	Type	u_a ($\times 10^3$) u_c ($\times 10^3$)	T_{11}	T_{22}	T_{33}	T_{12}	T_{13}	T_{23}	R ($\times 10^3$) wR ($\times 10^3$)	K_1	σ	Distribution	Model‡
*LINEX*74	7	I	102 (12) 151 (5)	not positive-definite						34 42	139·8 ±4·4	2·27	Gaussian	CH
	8	I	102 (5) 154 (2)	491·5 ±40·2	430·0 ±43·6	34·8 ±1·6	−239 ±37	−4·6 ±9·2	−1·4 ±9·1	18 23	139·1 ±2·0	1·12	Gaussian	TN
	9	I	110 (12) 161 (7)	0·0078 ±0·0036	0·0006 ±0·0078	0·0779 ±0·0282	0·0015 ±0·0070	−0·0026 ±0·0050	−0·0015 ±0·0050	34 40	153·2 ±6·9	2·18	Lorentzian	CH
	10	I	102 (6) 161 (4)	127·4 ±23·9	116·0 ±23·4	9·1 ±1·4	−60·8 ±14·1	−1·3 ±2·4	−0·34 ±2·4	15 22	148·5 ±3·0	1·18	Lorentzian	TN
	11	II	097 (4) 157 (3)	11·6 ±3·0	11·9 ±3·0	736 ±197	−6·0 ±1·9	+6·0 ±10	−1·2 ±10	22 30	139·9 −0·9	1·58	Gaussian	–

* With or without inclusion of the Borrmann effect.
† Principal axes and direction cosines. $a \times 10^3 = r_{ii}$ in Å.
‡ Model of anisotropic extinction used: CH – Coppens & Hamilton; TN – Thornley & Nelmes.

Table 5. Mo *data*: *results of refinement for different anisotropic extinction correction models*

T_{ij}: tensor components Z_{ij}, W_{ij}, Y_{ij} and E_{ij} respectively.

Program used	No.	Type	u_a ($\times 10^3$) u_c ($\times 10^3$)	T_{11}	T_{22}	T_{33}	T_{12}	T_{13}	T_{23}	R ($\times 10^3$) wR ($\times 10^3$)	K_1	σ	B.E.*	Using (2) or (3)
ORXFLS3	12	I	111 (5) 174 (5)	not positive-definite						30 41	63·5 ±3·1	3·4	yes	(2)
	13	I	100 (10) 162 (1)	not positive-definite						9 11	54·8 ±0·4	0·9	no	(2)
	14	II	112 (4) 173 (4)	0·72 ±0·30	0·56 ±0·25	1·30 ±0·57	−0·49 ±0·23	0·13 ±0·14	−0·05 ±0·13	30 36	63·9 ±2·9	3·0	yes	(2)
	15	II	111 (4) 174 (5)	0·74 ±0·30	0·56 ±0·29	1·44 ±0·75	−0·49 ±0·28	0·13 ±0·19	−0·22 ±0·21	36 44	64·4 ±3·4	3·6	yes	(3)
	16	II	101 (1) 163 (1)	9·66 ±1·31	10·0 ±1·2	84·4 ±9·5	−1·4 ±1·3	1·0 ±2·1	−8·1 ±2·5	7 8	55·2 ±0·3	0·7	no	(2)
				2·5 (2) 2·2 (2) 0·8 (1)	−0·64 0·77 −0·02	0·77 0·63 −0·11	0·07† 0·08 0·99							
	17	II	101 (1) 162 (1)	11·0 ±1·4	11·3 ±1·2	94·4 ±10·1	−2·1 ±1·3	1·4 ±2·1	−8·6 ±2·5	6 8	55·1 ±0·3	0·7	no	(3)
				2·4 (2) 2·0 (2) 0·7 (1)	−0·65 0·75 −0·02	0·75 0·64 0·10	0·07† 0·08 0·99							

Program used	No.	Type	u_a ($\times 10^3$) u_c ($\times 10^3$)	T_{11}	T_{22}	T_{33}	T_{12}	T_{13}	T_{23}	R ($\times 10^3$) wR ($\times 10^3$)	K_1	σ	Distribution	Model‡
LINEX74	18	I	not convergent										Gaussian	CH
	19	I	96 (1) 159 (1)	216·8 ±46·0	401·4 ±77·2	24·8 ±1·3	−143 ±58	−13 ±10	−13 ±16	8 10	53·7 ±0·2	0·8	Gaussian	TN
	20	I	not convergent										Lorentzian	CH
	21	I	98 (1) 161 (1)	77·4 ±13·6	157·4 ±28·8	11·17 ±0·40	−87·4 ±19·5	−6·8 ±3·5	−4·1 ±5·3	7 8	54·9 ±0·2	0·6	Lorentzian	TN
	22	II	96 (3) 161 (1)	not positive-definite						14 19	54·7 ±0·7	1·6	Gaussian	–

* With or without inclusion of the Borrmann effect.
† Principal axes and direction cosines. $a \times 10^3 = r_{ii}$ in Å.
‡ Model of anisotropic extinction used: CH – Coppens & Hamilton; TN – Thornley & Nelmes.

obtained in refining all six extinction parameters without constraints show that the ellipsoids describing the mean shape of the mosaic blocks almost take on the symmetry of the crystal lattice (see r_{ii} and the direction cosines in Tables 4 and 5). The ellipsoid describing the anisotropy of the block size for calculation (6) in Table 4 is illustrated in Fig. 1(*a*) and (*b*), drawn by the program for illustration of the thermal vibration ellipsoids, *ORTEP* by Johnson (1965). The other ellipsoids for Cu and Mo measurements have similar shapes and orientations, but different values for the lengths of the principal axes.

For all type II model calculations the principal axes of the mean domain block ellipsoids in the basal plane, r_{11} and r_{22}, are nearly equal in length and three to four times larger than r_{33} in the direction of the *c* axis, indicating that the atoms prefer to build up the basal plane more rapidly than the lattice in the *c* direction.

Zachariasen (1968*a*) pointed out that for mosaic crystals with spherical domain blocks and of intermediate type it is possible to calculate the quantities *r* and *g*, characteristic for the crystal specimen, if measurements are made with two different wavelengths. For the intermediate mosaic crystal type Zachariasen's (1968*a*) result is:

$$r = r^*_{\mathrm{Mo}} r^*_{\mathrm{Cu}} [(\lambda^2_{\mathrm{Cu}} - \lambda^2_{\mathrm{Mo}})/(\lambda^2_{\mathrm{Cu}} r^{*2}_{\mathrm{Mo}} - \lambda^2_{\mathrm{Mo}} r^{*2}_{\mathrm{Cu}})]^{1/2}$$

$$g = (r^*_{\mathrm{Cu}} r^*_{\mathrm{Mo}})/(\lambda_{\mathrm{Cu}} \lambda_{\mathrm{Mo}}) \cdot [(\lambda^2_{\mathrm{Cu}} - \lambda^2_{\mathrm{Mo}})/(r^{*2}_{\mathrm{Cu}} - r^{*2}_{\mathrm{Mo}})]^{1/2}$$

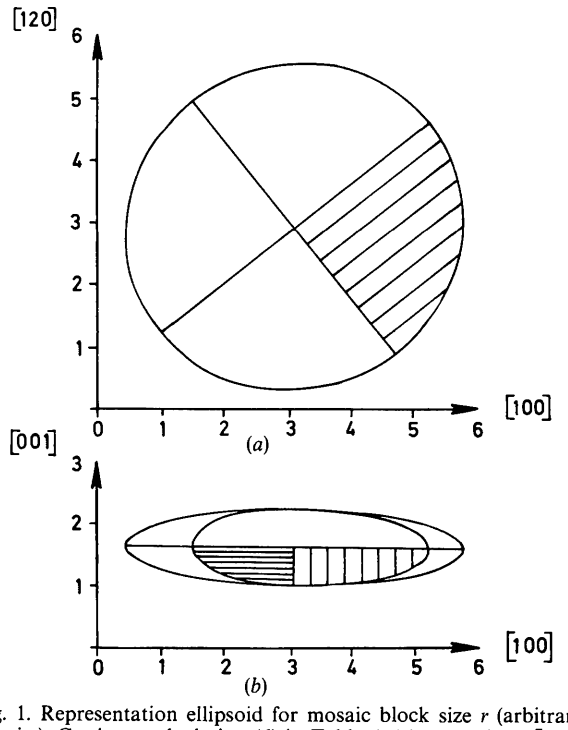

Fig. 1. Representation ellipsoid for mosaic block size *r* (arbitrary units). Cu data: calculation (6) in Table 4. (*a*) Axes along [100] and [120] of the hexagonal lattice. (*b*) Axes along [100] and [001] of the hexagonal lattice.

where

$$r^* = r(1 + (r/\lambda g)^2)^{-1/2} .$$

It is seen that the ratio $r^*_{\mathrm{Mo}}/r^*_{\mathrm{Cu}}$ must lie between the theoretical limits of $\lambda_{\mathrm{Mo}}/\lambda_{\mathrm{Cu}} = 0{\cdot}46$ and unity. For type I crystals it follows, that with $r^*_{\mathrm{Cu}} = \lambda_{\mathrm{Cu}} g$ and $r^*_{\mathrm{Mo}} = \lambda_{\mathrm{Mo}} g$, $r^*_{\mathrm{Cu}}/r^*_{\mathrm{Mo}} = \lambda_{\mathrm{Cu}}/\lambda_{\mathrm{Mo}}$, *r* cannot be determined and $g = r^*/\lambda$.

For type II crystals $r^*_{\mathrm{Mo}} = r$ and $r^*_{\mathrm{Cu}} = r$ and therefore $r^*_{\mathrm{Mo}} = r^*_{\mathrm{Cu}}$. Therefore *g* cannot be determined. An attempt to use Zachariasen's formulae was made in the directions of the *a* and *c* axes of the extinction ellipsoid using the results for r_{ii} from the calculations (6) and (17) in Tables 4 and 5. For type II crystals, (in calculating r^* in this example it was assumed that the crystal is of type II) r^*_{Mo} should equal r^*_{Cu}. Neither for the *a* direction nor for the *c* direction is this statement true.

If we assume that we have a crystal of intermediate type, then $r^*_{\mathrm{Mo}}/r^*_{\mathrm{Cu}}$ must lie between 0·46 and unity and *r* and *g* can be calculated. However, this condition is not fulfilled, neither for the *a* direction ($r^*_{\mathrm{Mo},a}/r^*_{\mathrm{Cu},a} \sim 2200/7450 \sim 0{\cdot}30$) nor for the *c* direction ($r^*_{\mathrm{Mo},c}/r^*_{\mathrm{Cu},c} \sim 700/1800 \sim 0{\cdot}39$).

Because of these problems it was felt that the extinction correction in *ORXFLS*3 is unsatisfactory for the Zn sample, although modifications have been made to include the Borrmann effect and the polarization of the incident beam. The intensity data were therefore refined once again, with the least-squares program *LINEX* 74.

(*b*) *The results of refinement with LINEX* 74

In *LINEX* 74 the formulae for *y* of Becker & Coppens (1974) (Table 2) together with formula (1) are used. All four models for anisotropy given in Table 3 for type I crystals can be refined. For type II crystals the tensor components E_{ij} defined by Becker & Coppens (1975) (Table 3) are used. The tensor components are given in a system with axes parallel to the real crystal axes.

The results of refinement for type I and type II models with *LINEX* 74 are shown in the second parts of Tables 4 and 5 for Cu data and Mo data respectively.

From Tables 4 and 5 the following conclusions can be drawn. Lower *R* values are obtained with *LINEX* 74 than with *ORXFLS*3, especially for Cu data. The *Y*(obs)–*Y*(cal) lists calculated with *LINEX* 74 show better agreement than those of *ORXFLS*3, which show systematic disagreement for *Y* values with small $\sin\theta/\lambda$. Because the Mo data do not yield positive-definite parameters for type II and because the *R* value for type II is higher than that of the best fitted type I model for Cu data, it can be concluded that the extinction is dominated by mosaic spread in the Zn sample.

With the Thornley–Nelmes anisotropy model better agreement was obtained than with the Coppens–Hamilton's model, for which the LSQ was divergent

in the case of Mo and leads to non-positive-definite parameters in the case of Cu data, if a Gaussian distribution is assumed. The Lorentzian distribution seems to fit the data better than the Gaussian distribution for both Mo and Cu. These results are in agreement with the general conclusions of Becker & Coppens (1975) and Thornley & Nelmes (1974). The best fit with *LINEX* 74 was obtained for the type I model, assuming Lorentzian distribution for the mosaic spread and the Thornley & Nelmes (1974) model for anisotropy. The Y(cal)–Y(obs) lists for this fit are given in the Table 7(*a*) for the Cu data and 7(*b*) for the Mo data, showing good agreement between observed and calculated structure factors.†

The root-mean-square displacement of Zn

With

$$u_a=(\beta_{11}/2\pi^2 a_1^{*2})^{1/2} \text{ and } u_c=(\beta_{33}/2\pi^2 a_3^{*2})^{1/2}$$

the root-mean-square displacements in directions **a** and **c** of the h.c.p. lattice were calculated. The values are tabulated in the fourth columns of Tables 4 and 5, for the different anisotropic extinction models used. In Table 6 the values of u_a, u_c and R for the best fit (*LINEX* 74, type I, Lorentzian distribution, Thornley & Nelmes) are collected together with the values for the calculations with isotropic extinction and those without extinction taken into account.

Table 6. *Comparison of the root-mean-square displacement for calculations with anisotropic and isotropic extinction and without extinction*

All values are multiplied by a factor of 10^3.

	Without extinction correction			With isotropic extinction correction			With anisotropic extinction correction		
	R	u_a (Å)	u_c (Å)	R	u_a (Å)	u_c (Å)	R	u_a (Å)	u_c (Å)
Cu	82	Non-positive-definite		49	104 (2)	143 (2)	15	102 (6)	161 (4)
Mo	64	60 (30)	130 (30)	26	101 (1)	157 (1)	7	98 (1)	161 (1)

From Tables 4, 5, 6 and 7 the following conclusions can be drawn:

1. Neglect of the extinction correction results in low values for u_a and u_c for the Mo data, in accordance with the statement made in the *Introduction*. For Cu data, where the extinction is more severe, non-positive-definite temperature factors result. The Y(obs)–Y(cal) lists in Table 7 show high disagreement between measured and calculated intensities, resulting in a high R value.

2. The results for u_a and u_c, when an anisotropic extinction correction is made, are in good agreement with those of Skelton & Katz (Table 1), showing that if extinction correction is properly used it is possible to get significant temperature factors with the help of least-squares analysis.

3. If the calculations including the Borrmann effect and those which result in non-positive-definite extinction parameters are ignored, Tables 4 and 5 show that the results for u_a and u_c are nearly independent of the anisotropic extinction model used.

† Table 7 has been deposited with the British Library Lending Division as Supplementary Publication No. SUP 32540 (5 pp.). Copies may be obtained through The Executive Secretary, International Union of Crystallography, 13 White Friars, Chester CH1 1NZ, England.

APPENDIX

Glossary of symbols

A	the transmission factor
A^*	the absorption factor
$A(\theta), B(\theta)$	least-squares-fitted coefficients occurring in the expression for y (Becker & Coppens, 1974)
a, b, c	unit-cell dimensions
a_i^*	reciprocal-lattice constants
D	unit vector normal to the diffraction plane
E	second-order tensor defined in Table 3
e^2/mc^2	electron radius
$\exp(-M)$	temperature factor
F	structure factor
f_j	form factor of the jth atom
g	width parameter of the mosaic distribution
g^*	extinction parameter defined in Table 2
h	reciprocal vector
hkl	Miller indices
I	measured integrated intensity corrected for absorption and Lp
I_m	measured integrated intensity
I_k	intensity in kinematical approach
K	the coefficient of polarization: 1 for the parallel component of the X-ray electric field; $\lvert\cos 2\theta\rvert$ for the perpendicular component of the X-ray electric field
K_1	scale factor in least-squares analysis
N	unit vector which lies in the diffraction plane and is perpendicular to the incident beam
N_o	number of observations
N_v	number of variables to be varied
P	term describing the polarization of the X-ray electric field
Q_0	$=[(e^2/mc^2)^2F^2\lambda^3]/(V^2 \sin 2\theta)$
r	mean radius of the spherical mosaic domain blocks
r_{ii}	principal axes of the representation ellipsoid for the mosaic block size
$\mathbf{r}_j$	vector from the origin of the unit cell to the jth atom
r^*	$=r[1+(r/\lambda g)^2]^{-1/2}$

R	$=\Sigma\lvert Y(\text{obs})-Y(\text{cal})\rvert/\Sigma Y(\text{obs})$
R_s	radius of the spherical Zn sample
SIG	$=(\Delta I/2\sqrt{I_m}).A^*/(K_1.\sqrt{y})$
$\overline{T}$	mean path length through the crystal
$\overline{T}$	absorption-weighted mean path length through the crystal
u	unit vector parallel to the direction of the incident beam
u_a, u_c	root-mean-square displacements in a and c directions of the lattice
V	volume of the unit cell
wR	$=\{\Sigma(1/\text{SIG}).[Y(\text{obs})-Y(\text{cal})]^2\}^{1/2} \div[\Sigma(1/\text{SIG}).Y(\text{obs})^2]^{1/2}$
W	second-order tensor defined in Table 3
x_j, y_j, z_j	positional parameters of the jth atom in the unit cell
y	extinction correction
$y_{\parallel}, y_{\perp}$	extinction correction for the parallel or perpendicular component of the X-ray electric field
$Y(\text{obs})$	$=\sqrt{I_m}A^*/(K_1.\sqrt{y})$
$Y(\text{cal})$	$=\sum_j f_j \exp(2\pi\mathbf{hr}_j)\exp(-M)$
Y	second-order tensor defined in Table 3
Z	second-order tensor defined in Table 3
α	significance level of Hamilton's R-ratio test
β_{ij}	anisotropic temperature factors
ΔI	error in I_m, with the variance from counting statistics and systematic errors of the measurement [filter-factor error, discrepancies in reference measurements (measured several times during the measurement of the Bragg intensities)] taken into account
η	mosaic spread parameter
θ, θ_m	Bragg angle of the sample and monochromator respectively
λ	wavelength of the radiation
$\lambda_{\text{Mo}}, \lambda_{\text{Cu}}$	wavelengths for Mo and Cu radiations
μ_0	linear absorption coefficient
μ_{ij}	atomic absorption coefficient of the jth atom in the unit cell
μ	absorption coefficient defined in (4)
σ	$\Sigma(1/\text{SIG}).[Y(\text{obs})-Y(\text{cal})]^2/(N_o-N_v)$

References

ABRAHAMS, S. C., ALEXANDER, L. E., FURNAS, T. C., HAMILTON, W. C., LADELL, J., OKAYA, Y., YOUNG, R. A. & ZALKIN, A. (1967). *Acta Cryst.* **22**, 1–6.

ABRAHAMS, S. C., HAMILTON, W. C. & MATHIESON, A. McL. (1970). *Acta Cryst.* A**26**, 1–18.

AZAROFF, L. (1955). *Acta Cryst.* **8**, 701–704.

BECKER, P. & COPPENS, P. (1974). *Acta Cryst.* A**30**, 129–147.

BECKER, P. & COPPENS, P. (1975). *Acta Cryst.* A**31**, 417–425.

BRINDLEY, M. S. (1936). *Phil. Mag.* **21**, 790–808.

BUSING, W. R., MARTIN, K. O. & LEVY, H. A. (1962). *ORFLS.* Report ORNL-TM-305, Oak Ridge National Laboratory, Tennessee.

COPPENS, P. & HAMILTON, W. C. (1970). *Acta Cryst.* A**26**, 71–83.

CROMER, D. T. & LIBERMAN, D. (1970). *J. Chem. Phys.* **53**, 1891–1898.

CROMER, D. T. & MANN, J. B. (1968). *Acta Cryst.* A**24**, 321–342.

GUSE, W. (1971). *Über die Herstellung metallischer Teilchen im Grössenbereich des Staubes.* Thesis, Univ. Hamburg, BRD.

HAMILTON, W. C. (1965). *Acta Cryst.* **18**, 502–510.

HAMILTON, W. C. & ABRAHAMS, S. C. (1970). *Acta Cryst.* A**26**, 18–24.

JAUNCEY, G. E. M. & BRUCE, W. A. (1936). *Phys. Rev.* **50**, 408–412.

JOHNSON, C. K. (1965). *ORTEP.* Report ORNL-3794, Oak Ridge National Laboratory, Tennessee.

LYNCH, R. W. & DRICKAMER, H. G. (1965). *J. Phys. Chem. Solids*, **26**, 63–68.

MERLINI, A. & PACE, S. (1965). *Nuovo Cim.* **35**, 377–390.

PETERSE, W. J. A. M. & PALM, J. H. (1966). *Acta Cryst.* **20**, 147–150.

RYBA, E. (1960). *Measurement of the Mean-Square Vibration Amplitude of Atoms in Metals by X-ray Techniques.* Thesis, Iowa State Univ.

SKELTON, E. & KATZ, L. (1968). *Phys. Rev.* **171**, 801–808.

THORNLEY, F. R. & NELMES, R. J. (1974). *Acta Cryst.* A**30**, 748–757.

WEBER, K. (1969). *Acta Cryst.* B**25**, 1174–1178.

WILLIS, B. T. M. & PRYOR, A. W. (1975). *Thermal Vibration in Crystallography*, pp. 135–137. Cambridge Univ. Press.

WOLLAN, E. O. & HARVEY, G. G. (1937). *Phys. Rev.* **51**, 1054–1061.

ZACHARIASEN, W. H. (1967). *Acta Cryst.* **23**, 558–564.

ZACHARIASEN, W. H. (1968*a*). *Acta Cryst.* A**24**, 212–216.

ZACHARIASEN, W. H. (1968*b*). *Acta Cryst.* A**24**, 421–424.

ZENER, C. (1936). *Phys. Rev.* **49**, 122–127.